Remote Sensing of Environment 114 (2010) 1638–1648

Contents lists available at ScienceDirect

Remote Sensing of Environment

journal homepage: www.elsevier.com/locate/rse

Reconstructing long time series of burned areas in arid grasslands of southern Russia by satellite remote sensing

Maxim Dubinin [a,*], Peter Potapov [b], Anna Lushchekina [c], Volker C. Radeloff [a]

[a] Department of Forest and Wildlife Ecology, University of Wisconsin — Madison, 1630 Linden Drive, Madison, WI, 53706, USA
[b] Geographic Information Science Center of Excellence, South Dakota State University, Wecota Hall, Box 506B, Brookings, SD 57007, USA
[c] Institute of Ecology and Evolution, Russian Academy of Sciences, 33 Leninskiy prospect, Moscow, 119071 Russia

ARTICLE INFO

Article history:
Received 4 September 2009
Received in revised form 28 January 2010
Accepted 13 February 2010

Keywords:
AVHRR
MODIS
RESURS
Landsat
Burned area mapping
Southern Russia
Arid grasslands
Grazing

ABSTRACT

Fire is an important natural disturbance process in many ecosystems, but humans can irrevocably change natural fire regimes. Quantifying long-term change in fire regimes is important to understand the driving forces of changes in fire dynamics, and the implications of fire regime changes for ecosystem ecology. However, assessing fire regime changes is challenging, especially in grasslands because of high intra- and inter-annual variation of the vegetation and temporally sparse satellite data in many regions of the world. The breakdown of the Soviet Union in 1991 caused substantial socioeconomic changes and a decrease in grazing pressure in Russia's arid grasslands, but how this affected grassland fires is unknown. Our research goal was to assess annual burned area in the grasslands of southern Russia before and after the breakdown. Our study area covers 19,000 km^2 in the Republic of Kalmykia in southern Russia in the arid grasslands of the Caspian plains. We estimated annual burned area from 1985 to 2007 by classifying AVHRR data using decision tree algorithm, and validated the results with RESURS, Landsat and MODIS data. Our results showed a substantial increase in burned area, from almost none in the 1980s to more than 20% of the total study area burned in both 2006 and 2007. Burned area started to increase around 1998 and has continued to increase, albeit with high fluctuations among years. We suggest that it took several years after livestock numbers decreased in the beginning of the 1990s for vegetation to recover, to build up enough fuel, and to reach a threshold of connectivity that could sustain large fires. Our burned area detection algorithm was effective, and captured burned areas even with incomplete annual AVHRR data. Validation results showed 68% producer's and 56% user's accuracy. Lack of frequent AVHRR data is a common problem and our burned area detection approach may also be suitable in other parts of the world with comparable ecosystems and similar AVHRR data limitations. In our case, AVHRR data were the only satellite imagery available far enough back in time to reveal marked increases in fire regimes in southern Russia before and after the breakdown of the Soviet Union.

1. Introduction

Fire is one of the main disturbance agents in grasslands and savannahs. Fire shapes vegetation structure and composition, and represents an important land-management tool (Pyne, 1984). Grasslands, woody savannahs, and savannahs represent more than 60% of the global burned area (Tansey et al., 2004), and in regions with high aridity, such as Central Asia, grassland fires account for 80% of all active fire counts (Csiszar et al., 2005). Fuel loads and emissions from grassland burning are relatively small (van der Werf et al., 2006), but grassland fires can foster the spread of invasive species (Brooks et al., 2004), affect wildlife (Archibald & Bond, 2004), and cause air pollution that can spread as far as the Arctic (Stohl et al., 2007). Furthermore, interactions between grassland fires and human land use may result in ecosystem degradation, hydrologic changes, soil disturbance, and shrub encroachment (Archer et al., 1995). The restoration, conservation and management of arid grasslands thus require solid information on their fire regime and its change over time. Our goal here was to assess fire regime changes in the grasslands of southern Russia before and after the breakdown of the Soviet Union.

Fire regimes in general are largely determined by fuel moisture, fuel amount, and ignition sources (Bond & van Wilgen, 1996). Arid grasslands are biomass-poor, and at least seasonally dry ecosystems, in which fuel amount and connectivity are the main limiting factors for fires (Meyn et al., 2007). Climate change can cause long-term changes in fuel amounts, but land use affects fuel amounts more directly and acutely. The main control of fuel amount in many arid grasslands is livestock (Bahre, 1991). Unlike mesic grasslands, which evolved with intensive mammalian herbivory, arid grasslands are

* Corresponding author.
E-mail address: dubinin@wisc.edu (M. Dubinin).

0034-4257/$ – see front matter © 2010 Elsevier Inc. All rights reserved.
doi:10.1016/j.rse.2010.02.010

more sensitive to livestock grazing (Mack & Thompson, 1982) often leading to overexploitation and degradation (Akiyama & Kawamura, 2007; Zhang et al., 2007). Vegetation can recover when livestock grazing decreases, and the resulting increase in fuel amounts and connectivity may be able to sustain extensive wildfires (Liedloff et al., 2001). However, fire increases resulting from a decrease in livestock grazing have rarely been studied, and the long-term relationship between livestock grazing, burning dynamics, and environmental factors is not well understood. Thus, it is often inappropriate to study livestock-fire relationships with small plots and difficult to employ a classical experimental design at such broad temporal and spatial scales.

Where controlled experiments are impossible, natural experiments may offer insights (Diamond, 2001). Significant socioeconomic disruptions and the resulting land-use changes can provide natural experiments to study accompanying environmental changes (Kuemmerle et al., 2007). Land-use change research typically examines how socioeconomics affect land use directly (Lambin & Geist, 2006). However, it may be that indirect cascading effects, such as alterations of disturbance regimes, have a much larger effect on the ecosystem (Burcher et al., 2007). In the context of livestock grazing and grassland fires, the ideal natural experiment would comprise a strong decrease in livestock grazing, sufficient time for the resulting changes in fire regimes to manifest themselves, and relatively constant conditions for all other relevant factors. The breakdown of the Soviet Union in 1991 provided such a natural experiment.

The former Soviet Union including Russia experienced dramatic changes in livestock population in the arid grasslands, such as in the Republic of Kalmykia (Fig. 1). In the early 1970s, under state-controlled plan-based economic policies, sheep numbers more than doubled, and stayed at over 800 thousand heads for about twenty years. During these years, the bulk of sheep industry was represented by large agricultural enterprises, which overexploited the grasslands. Grazing intensified up to a point where some pastures were grazed year-round. Intensive grazing caused widespread wind erosion and vegetation degradation (Zonn, 1995). Due to overgrazing, southern Russia was called “Europe's first anthropogenic desert” in the mid 1990s (Saiko & Zonn, 1997). Some model forecasts predicted that even with protection, more than 66% of southern Russia's grassland would convert to bare sand by 2000 (Vinogradov, 1995), and substantial governmental action was taken to combat desertification.

However, following the breakdown of the USSR in 1991 livestock populations dropped by almost an order of magnitude (Fig. 1) and remained low until around 2000 (Brooks & Gardner, 2004; ROSSTAT, 2007). Large collective and state-owned farms were no longer subsidized after 1991, resulting in broad-scale de-collectivization and abandonment. The livestock decline allowed vegetation to recover and may thus have caused potentially an increase of grassy fuels. Thus the hypothesis is that the decrease in grazing pressure resulted in an increase in grassy fuels, and ultimately in an increase in grassland fires. The problem is that no fire data are readily available to test this hypothesis since official fire records for the region, similar to other regions are incomplete and inaccurate (Soja et al., 2004).

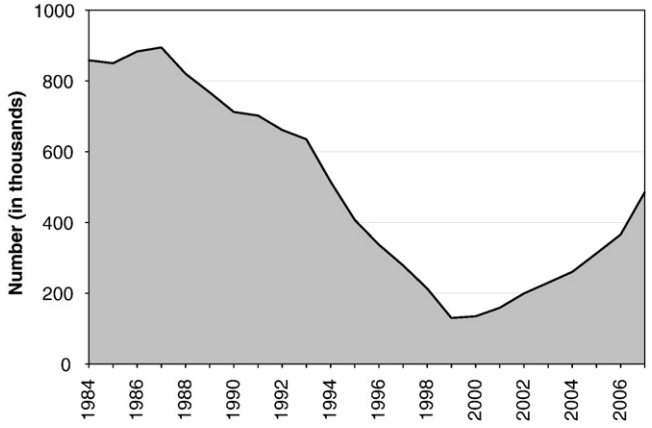

Fig. 1. Total sheep population in three administrative regions of the Republic of Kalmykia (Chernozemelsky, Iki-Burulsky, Lagansky) which closely correspond to the boundaries of our study area (ROSSTAT, 2003, 2007).

Remote sensing and satellite data have been used for more than 20 years to monitor fires in many different parts of the world (Csiszar et al., 2004). Coarse-resolution satellite data are one of the best sources for historic burned area mapping because of their high temporal resolution and long history of acquisitions (Arino et al., 2001). Two basic types of algorithms exist to estimate fire affected areas from Advanced Very High Resolution Radiometer (AVHRR) or Moderate-Resolution Imaging Spectroradiometer (MODIS) data: a) detection of active fires, and b) mapping burn scars or burned areas. Though area burned correlates well with the number of fires, deriving burned areas from active fire detections is error prone, especially in some ecosystems, because the detected hotspots can underestimate the actual burned area (Giglio et al., 2006; Hawbaker et al., 2008; Miettinen et al., 2007). In contrast, burned area assessments identify postfire disturbance, but not the actual fire event.

Typically, burned area mapping involves band differencing and thresholding or classifying single or multitemporal data in the form of raw band values and derivative indices (Arino et al., 2001; Gong et al., 2006; Kučera et al., 2005). Burned area maps from coarse spatial resolution data are prone to several types of errors: low resolution bias, lack of imagery in certain areas, and geometric and radiometric errors (Barbosa et al., 1999; Boschetti et al., 2004). Most of these problems are more prevalent in AVHRR data, and have been solved or notably reduced in recent sensors such as MODIS on board of Terra and Aqua. However, MODIS images are only available since 2000 and this relatively short time series limits the analysis of long-term trends. Thus AVHRR remains the only remote sensing dataset capable of reconstructing long-term (20+ years) burning trends (Chuvieco et al., 2008; Kučera et al., 2005) at regional scale. The classification of satellite images for burned area mapping typically requires regular AVHRR observations, composited from daily data. Full resolution AVHRR data (Local Area Coverage, LAC, or High Resolution Picture Transmission, HRPT, both at 1.1 km at nadir) greatly improves the classification of burned areas (Pu et al., 2007; Razafimpanilo et al., 1995; Sukhinin et al., 2004).

Unfortunately, the amount and quality of AVHRR data vary greatly among different regions. Daily AVHRR observations at 1.1 km spatial high resolution are not always available, especially for those parts of the world where local archives had not been established until the late 1990s. Southern Russia is one such area, and only a limited amount of AVHRR data is available in international archives such as NOAA's Comprehensive Large Array-data Stewardship System (CLASS, http://www.class.noaa.gov/saa/products/welcome). Because of the limited data availability, existing remote sensing methods designed to map burned areas from AVHRR data cannot be applied and there is a need to develop new approach to map burned areas in regions where only CLASS-type AVHRR data are available.

The main goal of this study was to assess changes in burning in the grasslands of southern Russia before and after the breakdown of the Soviet Union. Our hypothesis was that annual burned area increased substantially after the breakdown of the Soviet Union due to the decline of livestock populations and more abundant fuels. Our second goal was to develop and test a method to derive burned area trends from temporally sparse CLASS-type AVHRR data. Our study was motivated by 1) the absence of any solid information on distribution of fires throughout 1980s and '90s in the study area and throughout Central Asia, 2) substantial socioeconomic changes in the region providing a unique ‘natural experiment’ to examine the effects of decreasing livestock grazing on fire regimes, and 3) the need for a

remote sensing approach that can map long-term burned area trends in arid grasslands from sparse AVHRR data.

2. Methods

2.1. Study area

Our study area is located in the grasslands of Southern European Russia and occupies about 19,000 km^2 of the Republic of Kalmykia and Astrakhan Region (Fig. 2). The study area was defined in the west and east by the administrative boundaries of the Republic and in the north and south by the boundaries of the common area of available AVHRR overpasses. The study area is sparsely populated (population density 0.8 to 1.4 persons/km^2) (CIESIN & CIAT, 2005) with no expectation for population growth (CIESIN et al., 2005).

The climate of the study area is arid, with hot, dry summers (mean daily temperature of +24 °C in July; max +44 °C, 280 days of sunshine per year on average). Annual precipitation is 150 to 350 mm (with a mean of 286 mm for 1985 to 2007). Summer droughts are common, and most of the precipitation falls in spring (43% of all precipitation), coinciding with the period of most vegetation growth (Walter & Box, 1983). The topography of the study area is predominantly flat with a mean elevation of −15 m below sea level. The study area has a complex geological history of transgressions and regression of the Caspian Sea and soils characterized by a gradient from sandy aeolian deposits and sandy loams in the southeast corner of the study area to clay loam in northwest corner (Kroonenberg et al., 1997).

Vegetation associations are typical for northern Precaspian Plains and represent combinations of steppe and desert types. The main vegetation associations are shortgrass steppe (*Stipa* spp., *Festuca* spp., *Agropyron* spp., *Anizantha tectorum*, and other graminoids, Fig. 3) and sage scrub (*Artemisia* spp., *Kochia prostrate*, Fig. 3) (Golub, 1994). Shortgrass steppe is characterized by a short growing season in April and May and rapid senescence in the dry summer. The grasses exhibit fire adaptation due to dense bunches which protect seeds and generate abundant fuels for burning. Sagebrush (*Artemisia* spp.) dominated shrublands have less biomass, but a longer growing season, and sometimes exhibit a second vegetation peak in the fall or even early winter (Kurinova & Belousova, 1989). *Artemisia* spp. is more susceptible to fire because its buds are situated above ground and can be killed or damaged by fires. The lack of fire tolerance by *Artemisia* spp. might lead to its substitution by *Stipa* spp. and other graminoids. The primary human land use of the grasslands in the study area is as rangelands to support grazing for domestic livestock, mainly sheep and to a lesser extent cows and goats.

Fig. 2. Study area location (hatched polygon with black outline), gray line — Republic of Kalmykia; the grayscale background represents shaded relief (SRTM30).

2.2. Study period

We studied burned area dynamics from 1985 to 2007. The choice of the study period was determined by remote sensing data availability and because of significant changes in land use after 1991. The 23 year fire record that we derived is one of the longest for a burned area estimation with coarse-resolution satellite data. Other burned area studies have either focused on forests or analyzed smaller time spans while studies of equivalent time span are particularly rare (Chuvieco et al., 2008; Kučera et al., 2005).

2.3. Data

2.3.1. Classification data

We used coarse spatial resolution AVHRR level 1B imagery in the form of digital numbers to estimate burned areas and three types of coarse- and medium-resolution satellite imagery for validation. We chose AVHRR for our burned area time series, despite its limited spatial and spectral resolutions, because the length of the AVHRR data record matched our research goal to compare pre- and post 1991 burned areas. For the burned area classifications, we analyzed AVHRR LAC images acquired by the National Ocean and Atmospheric Administration (NOAA) satellites (9,11,14,16,17). LAC data are stored onboard the satellite and downloaded at one of the NOAA receiving stations. All daytime images from 1985 to 2007 were downloaded from NOAA's CLASS. From these data, we selected a subset of images ranging from April 1st to September 20th of each year, corresponding to the beginning and the end of the growing season, and fully capturing the time of summer droughts and thus the fire season. From all images for each year, two images were selected according to the following criteria: i) the sensor angle was less than 45° off nadir, ii) no clouds obscured the study area, iii) the first image represented the peak of the growing season or close to it (April, May, or early June), and iv) the second image represented the end of the dry season and the end of the fire season (late August to early September).

Typically, CLASS AVHRR LAC images covering whole study area were available for every second day of the study period. Most of the CLASS AVHRR LAC imagery had to be discarded though. For example, in 2006, for the key period from April to September (i.e., 173 days), 90 images were available. However, among those, 49 images had excessive cloud cover, 10 had scanner malfunction, and 29 were ≥45° off nadir for the study area. Among the 12 remaining images that were not discarded only 3 were available before the burning season (i.e., in May and early June) and 3 after the burning season (i.e., in August). The choice of our classification algorithm thus reflected in no small part the lack of frequent CLASS AVHRR LAC images for our study area.

We based our classification on the assumption that fires will raise reflectance, due to the removal of vegetation, and that after fire event brightness will remain elevated through the rest of the season. Persistent increase in brightness was confirmed by preliminary MODIS analyses (Fig. 4). Unfortunately, due to limitations in data availability, the dates of the AVHRR images were not identical among years. Image dates for the earlier image with the exception of 1998 (early April) were all from early May or the first week of June. Later image dates ranged from early (1994, 2000, and 2005) to late August and to early September. All satellite images were clipped to the study area boundaries.

The two selected images for each year were then composited into 12 bands, where bands 1–3 represented the AVHRR spectral bands

Fig. 3. Feathergrass (*Stipa* sp.) (top) and sage (*Artemisia* sp.) (bottom) dominated communities in the beginning (left) and the end (right) of the vegetation season.

from the spring image (620–670, 725–1100, 3550–3930 nm); 4–6 represented the AVHRR bands from the fall image; 7–9 were band differences where each fall band was subtracted from the corresponding spring band and offset value was added to avoid negative numbers; and 10–12 represented NDVI for the first and second images (NDVI1, NDVI2) and their difference (NDVI12). We removed band 5 as it was not present for all AVHRR instruments. Band 4 was removed from the classification after preliminary analysis showed that this band did not help differentiate burned from surrounding, non-burned areas. Dark object subtraction was used to correct the images radiometrically (Song et al., 2001). The minimum observed value was selected from the Caspian Sea, and we subtracted the digital number observed over clear water for each band from all pixel values in each respective band.

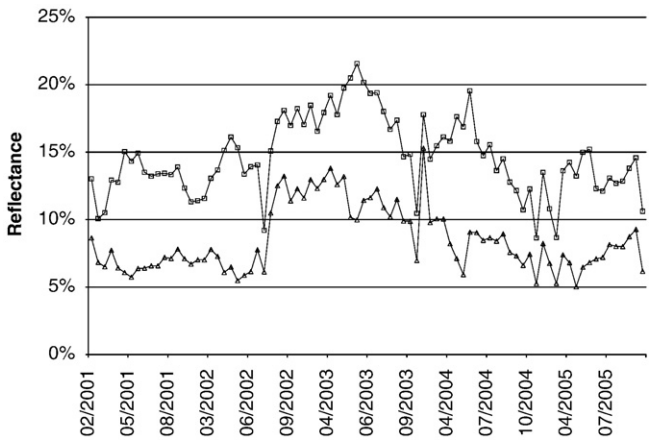

Fig. 4. 16-day MODIS reflectance values in bands 1 (triangles) and 2 (squares) for a sample area (median of 9 pixels) affected by fire (hatched line denotes the fire date). Winter-time snow contaminated values are not shown.

2.3.2. Validation data

For validation, we used Terra/Moderate-Resolution Imaging Spectroradiometer (MODIS), Landsat/Thematic Mapper (TM), Enhanced Thematic Mapper Plus (ETM+) and RESURS/Multi Spectral Scanner (MSU-SK) imagery. The MODIS Level 1B calibrated radiances product (MOD02QKM) with 250-m resolution was obtained from NASA's Level 1 and Atmosphere Archive and Distribution System (http://ladsweb.nascom.nasa.gov) and used for validation from 2000 to 2007. In addition to the validation, we also used MODIS data to estimate the temporal regime of burning (e.g., fire season length), because of MODIS' high temporal resolution. Landsat TM/ETM+ data were obtained from the USGS EROS Data Center at 30-m resolution for 1986 to 1989 and for 1999. Unfortunately, no TM/ETM+ data were available in either public (USGS GLOVIS) or commercial archives (Euroimage) for the period of 1990 to 1998. Instead we used RESURS MSU-SK data obtained from R&D center Scanex (http://scanex.ru) at 150-m resolution and 4 spectral bands ranging from 540 to 1175 nm for 1996 to 1998. All validation data was collected for the period correspondent to period of the AVHRR data that we used (i.e., April–September). Last but not least, we obtained official fire statistics (Ministry of Emergency). Although the official fire statistics do not include all burned areas, the statistics provided comparison for the recent years of the burned area time series.

2.4. Data processing

2.4.1. Geometric correction

For every year in the sequence, the first AVHRR image was co-registered to the MODIS image of June 7th 2008 with a second-order

polynomial transformation and nearest-neighbor resampling in ERDAS IMAGINE. The second image from a given classification pair was then co-registered to the first image using the same approach. The pixel size was set to 1.1 × 1.1 km. Semiautomatic tie point collection provided an initial set of ground control points (GCP). For each image from 7 to 10 GCPs were used for registration. Overall co-registration accuracy (root mean square error) was less than one pixel for each image. MODIS and Landsat data georeferencing accuracy is far superior to that of AVHRR and no additional georeferencing was necessary (Justice et al., 1998; Lee et al., 2004). Visual checking confirmed that the georeferencing of the validation data to the AVHRR data and 1:200,000 topographic maps was fine. RESURS data were co-registered to the June 7th 2008 MODIS image using the same methodology as for the AVHRR data. All imagery was reprojected to WGS84 coordinate system and equal-area Albers projection (central meridian at 45°, first standard parallel 52 and second standard parallel 64°).

2.4.2. Training data

Visual image interpretation provided training data for both burned and unburned areas for the classification. For each AVHRR image pair, a set of burned and non-burned areas was digitized. Burned areas were identified based on one of two possible features. Areas that had burned late in the season and were still black were characterized by lower reflectance in the fall image, especially in AVHRR band 2 (Pereira, 1999). Conversely, areas that had burned earlier in the season were highlighted by vegetation removal and a high proportion of bare ground, causing higher reflectance in bands 1 and 2 of the fall image. For every year, non-burned areas were also identified, including unburned vegetation, bare ground, and water bodies. All samples were combined into one comprehensive training dataset, which consisted of 11,706 pixels (2629 pixels for burned areas and 8447 for non-burned). We used a combined training dataset, rather than keeping training data for each year separate, because we could not detect any visible burned areas in the AVHRR images in the 1980s.

2.4.3. Classification

Our classification method had to account for the fact that there were major limitations in the AVHRR image availability (see above). We used decision tree classification to calculate the certainty that a given pixel burned in a given year. Decision trees are a robust approach to classify satellite data (Friedl & Brodley, 1997; Hansen et al., 2000) and are an effective tool for burned area mapping in grasslands (Maggi & Stroppiana, 2002; Stroppiana et al., 2003). Decision trees are nonparametric, i.e. no assumptions about the underlying distribution of the data are made, and decision trees can capture non-linear relationships between spectral data and different information classes (Breiman, 1984). To create more generalized and stable classification models we used a bagging approach (Breiman, 1996). Training data were sampled 30 times, each time extracting 15% of the comprehensive training dataset. Each selected sample was used to create a tree model resulting in an ensemble of 30 models. These models were applied to classify each of the 23 annual AVHRR data composites. The 30 classification results were then combined by averaging to estimate the probability of burning from 0 to 100%. Based on the probability, a simple majority threshold was used to tag the pixel as burned. Lastly, we used a 3 × 3 majority kernel to filter and

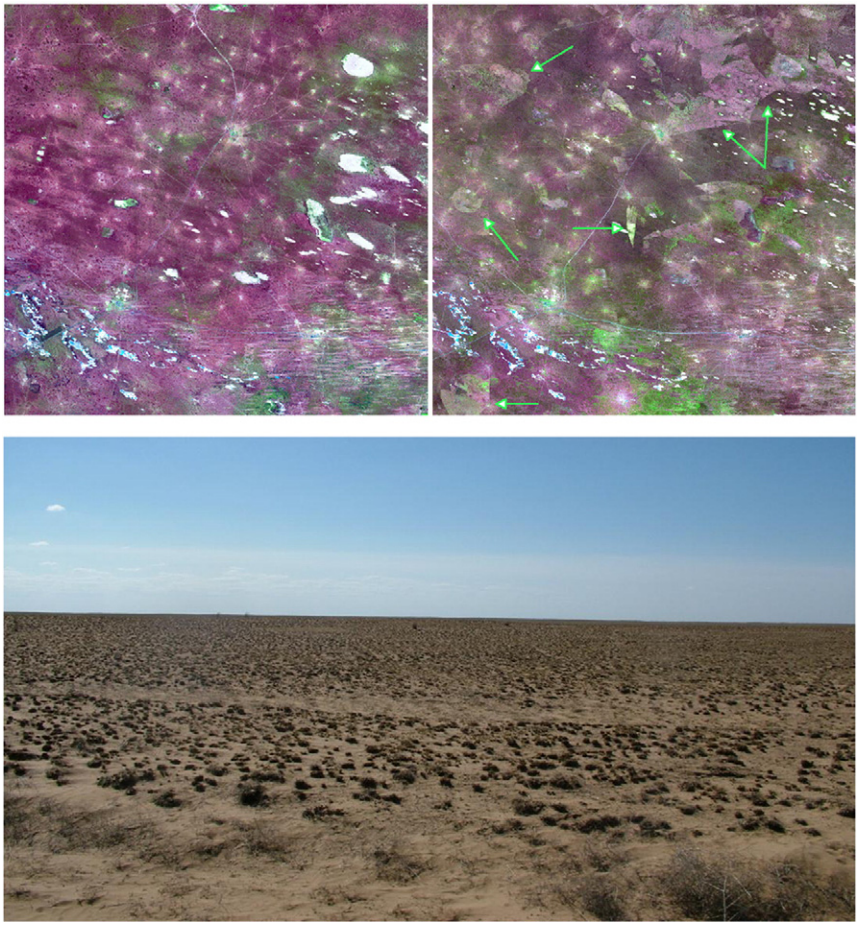

Fig. 5. Example of before-burning and after-burning in a Landsat TM image of September, 1988 and an ETM+ image of July, 2001 (5–4–3 band combination). Ubiquitous fire scars bounded by roads in the 2001 image, most of these scars are from previous years (marked with arrows). The photo represents an area burned in September, 4, 2005, photo taken March, 18, 2006.

smooth the classification results. This filtering may have removed some correctly mapped small fires, but we employed it to ensure conservative estimation of burned area and lower commission errors.

2.5. Validation

2.5.1. Burned area map validation

For the validation of the results we created an additional dataset of burned areas from higher-resolution imagery (TM, ETM+, MODIS, MSU-SK). Red–green–blue composites were created for each image, using bands 2 (841–876 nm), and 1 (620–670 nm) from MODIS, bands 5 (1550–1750 nm), 4 (760–900 nm), and 3 (630–690 nm) from TM/ETM+, and bands 4 (810–1000 nm), 2 (600–720 nm), and 1 (540–600 nm) from MSU-SK imagery. We validated our classifications for each year for which validation data were available.

Similarly to training data selection, validation data were obtained by visual image interpretation, shown to be at least as precise as automatic methods (Bowman et al., 2002). Delineating burned areas was straightforward due to distinct fire scar boundaries, often confined by linear features such as roads (Fig. 5). The easy recognition of fires was further facilitated by the lack of other disturbances in the area that could have resulted in comparable patterns. In many cases fire scars remained visible for 2 to 3 years after-burning, unless a new fire overrode an older scar (Fig. 5). The elevated brightness of burned areas was also quite stable intra-annually (Fig. 4). The validation dataset was rasterized to the 1.1×1.1 km pixels. Omission and commission errors were calculated for each year by combining binary burned classification and rasterized validation datasets. Producer's and user's accuracies were calculated from the four possible combinational classes (Congalton & Green, 1998). Additionally, we calculated the Kappa coefficient, which is a proportion of agreement obtained after removing the proportion of agreement expected to occur by chance (Congalton & Green, 1998).

2.5.2. Out of season validation

Because the AVHRR image dates were not uniform, we also checked if sub-optimal image dates caused omission of some fires. We tested this by comparison with numbers of active fire hotspots captured by both TERRA and AQUA satellites (MOD14A1 and MYD14A1). Based on the active fire data, we calculated the percentage of fires between August 20th and August 30th compared to the entire month of August, and the percentage of fires in August and September to the entire fire season for each year from 2000 to 2007. Though the number of active fire detections is correlated with the size of the burned area, this measure is not always reliable. Since some of the selected AVHRR images were collected in early August and we found some active fires in September that were not covered by the selected images, we extended the validation dataset until the end of September for the years 2002 to 2007. This allowed us to estimate how much burned area was missed due to the lack of optimally timed AVHRR images in some years.

2.5.3. Model transferability validation

Due to the coarse resolution of AVHRR satellite imagery, the visual estimation of training data may not always be reliable. Furthermore, in some years, no burned areas could be found for training. Using a comprehensive training dataset and a uniform set of decision tree models for all years captured the variability in burned area signals, and ensured that burning was not simply missed in a given year when visually interpreting the AVHRR data. However, the use of the comprehensive training dataset needed validation. To explore the transferability of the model to years for which there was no burned area training data, we removed training data for a set of years where amount of burning exceeded 15,000 km^2 (2000, 2002, and 2005 to 2007) from the comprehensive training dataset and repeated the classification. These tests quantified the extent to which uniform set of models was able to detect burning in one year in the absence of samples from this year in the comprehensive training set.

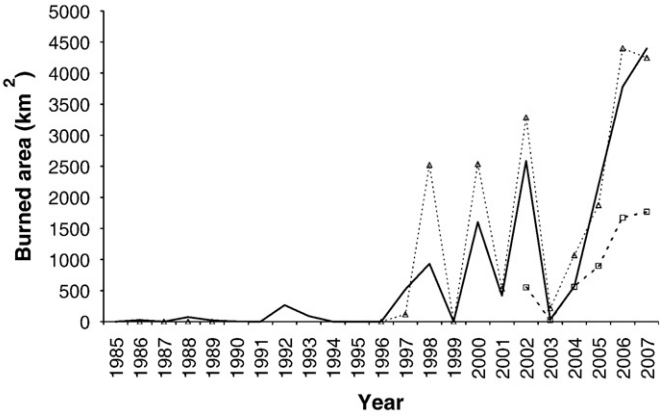

Fig. 6. Estimated burned area according to the AVHRR analysis (solid line), validation dataset (dotted line, triangles) and official burned area data (dashed line, squares).

3. Results

3.1. Annual burned area

Burned area increased dramatically from virtually no burning in the 1980s and the first half of the 1990s, to up to 19% of the study area (3600 km^2) burned annually after 2000 (Fig. 6 and Table 1). Among the 23 years that we studied, nine had substantial amounts of burned areas, while the other 14 had less than 2% of the area burned. Eight out of these nine high-burn years occurred after 1998 (Table 1). Large-scale burning started abruptly in 1997 and 1998, when 5% of the territory was burned and has continued regularly until today. However, burned area showed a high degree of variability, with one or two years of burning often followed by a year with negligible burned area.

Among the different AVHRR-derived bands that we used for the classification, the most important were the NDVI of the fall image and

Table 1
Annual burned area estimates and validation results.

Year	Burned area, km^2	Burned area % total	Producer's accuracy, burned	User's accuracy, burned	Producer's accuracy, non-burned	User's accuracy, non-burned	Kappa
1985	0	0.0	N/A	N/A	100.0%	100.0%	N/A
1986	25	0.1	0.0%	N/A	100.0%	99.9%	N/A
1987	0	0.0	0.0%	N/A	100.0%	98.7%	N/A
1988	74	0.4	0.0%	N/A	100.0%	99.6%	N/A
1989	21	0.1	0.0%	N/A	100.0%	99.9%	N/A
1990	4	0.0	N/A	N/A	100.0%	100.0%	N/A
1991	0	0.0	N/A	N/A	100.0%	99.5%	N/A
1992	266	1.4	N/A	N/A	100.0%	98.6%	N/A
1993	90	0.5	N/A	N/A	100.0%	99.5%	N/A
1994	0	0.0	N/A	N/A	100.0%	100.0%	N/A
1995	0	0.0	N/A	N/A	100.0%	99.8%	N/A
1996	0	0.0	0.0%	N/A	100.0%	99.4%	N/A
1997	518	2.7	18.5%	82.3%	99.9%	97.8%	29.4%
1998	933	4.9	92.5%	34.2%	90.8%	99.6%	46.1%
1999	0	0.0	0.0%	N/A	100.0%	99.9%	N/A
2000	1602	8.5	78.2%	48.9%	92.4%	97.9%	55.5%
2001	417	2.2	62.3%	28.4%	96.4%	99.1%	37.1%
2002	2586	13.7	82.6%	64.1%	92.7%	97.1%	67.2%
2003	34	0.2	28.2%	0.4%	82.5%	99.8%	1.7%
2004	567	3.0	67.8%	32.5%	95.6%	99.0%	41.4%
2005	2193	11.6	52.0%	63.5%	96.1%	93.8%	50.5%
2006	3781	20.0	86.5%	73.8%	92.3%	96.5%	74.2%
2007	4397	23.3	72.8%	75.4%	92.8%	91.8%	66.4%

the difference between spring and fall values of band 1 and band 3. These metrics explained 47% of the variability; each contributed respectively 24%, 14%, and 9% to the decrease of deviance for all 30 decision tree models. Other metrics were equally valuable and contributed on average 6% of the deviance decrease.

Large fires contributed to the majority of the burned area. As estimated using MODIS data, burns larger than 250 km^2 represented 48% of total burned area. Though small fires (less than 60 km^2) represented 77% of the total number of fires since 2000, their share accounted only for 18% of total burned area (Fig. 7). On average, the five largest fires in a given year represented 66% of the total burned area for that year. Since 2000, there was also a marked increase in the area of the largest fire, which grew from 58% of the total area burned in 2000 to almost 70% in 2006, and 71% in 2007 (1930, 3740, and 3120 km^2 respectively).

3.2. Validation

3.2.1. Burned area map validation

Validation of the burned area maps relied on data from different satellite sensors. For burned area delineations we used a total of 1066 MODIS images (a mean of 133 images per year, range 71–195), and 10 RESURS images (mean 3, range 2–4). MODIS data was available for the entire burning season; RESURS data also covered the entire burning season, except 1998, where the last RESURS image was acquired on August, 20th. Validation with Landsat data was based on September or late August imagery, and we used only one late season image per year. Average producer's accuracy of the burned area class in years where at least 200 km^2 burned was 68% (Table 1). Average user's accuracy for the same years was 56% (Table 1). The Kappa coefficient for the same year was 52% or moderate, according to classification scale by Congalton (1996). It was not possible to validate independently 10 out of 23 years (1985, 1990–1995) due to the lack of MODIS, Landsat, and RESURS data. No signs of burned areas were found for 7 of the validated years (1986, 1988, 1996, 1999, and 2003). Official statistics, available since 2002, were well correlated with the estimated trend, but showed generally much less burned area than our classifications (Fig. 6).

3.2.2. Temporal distribution and out of season validation

We estimated the temporal distribution of fires for 2000 to 2007 using MODIS active fire hotspots and our burned area boundaries derived for validation. As reported previously (Carmona-Moreno et al., 2005) burning predominantly started in June and ended in August (Fig. 8). Few active fire hotspots were detected before June and in late August and September. The percentage of active fire counts in August compared to a 3-month total was 26% (32% annual average),

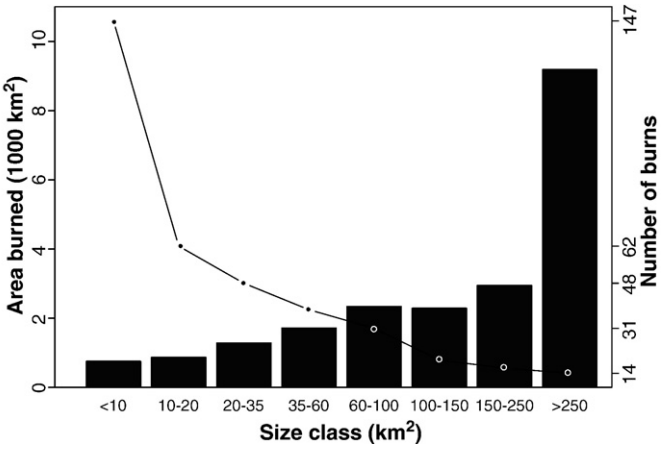

Fig. 7. Number (line) and area (bars) of burned areas from 2000 to 2007 summarized by size class.

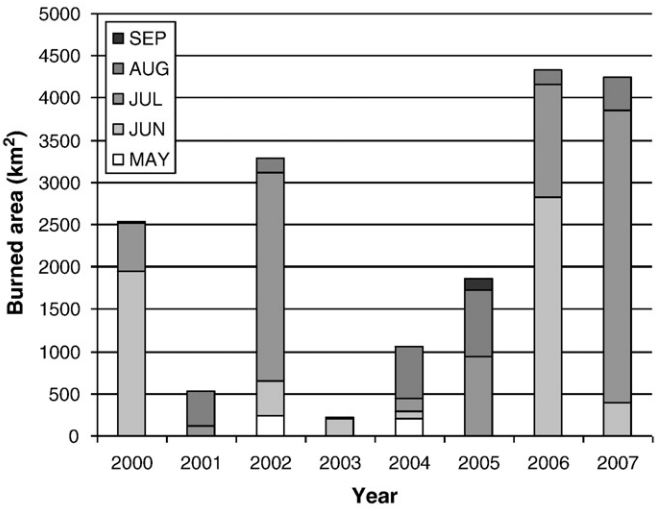

Fig. 8. Fire seasonality, i.e., the burned area by month, based on the MODIS image interpretation.

and only 9% (12% annual average) of the total number of active fires were detected in September. In August, most of the burning happened in the beginning and the middle of the month. The percentage of active fires detected during the last ten days of August was only 12% of the total number of active fire counts during August (14% annual average).

Burned areas mapped using MODIS data captured after the AVHRR images were taken showed that only a small proportion of burns were missed due to the timing of images. With the exception of 2003, less than 2% of total burned area occurred after the AVHRR images were taken (20 to 90 km^2 in a given years). However, in 2003 only 3 fires occurred in total, and one of those 3 occurred after the AVHRR image date and covered 70 km^2 or 63% of the total burned area in that year. Some burning may have taken place outside the windows captured by the AVHRR in those years for which no MODIS data were available. However, field observations, expert opinion and examination of imagery for period before and after fire season indicated that such burning was overall very limited.

3.2.3. Model transferability

We also tested how well our pooled training data could classify burns in years for which no training data were available (or withheld to test the transferability of the training data). Overall, the transferability was moderate. The amount of burned area for a particular year detected without training data from this year ranged from 84% (2002), 52% (2006), 44% (2007), down to as low as 17% (2005), of the area predicted with a full sample. Transferred models were successful in detecting burns that led to the complete removal of vegetation resulted in big areas of bare ground. Poor transferability in 2005 was likely due to a somewhat abnormal fire season. Unlike other test years, most of the burned areas in 2005 happened late in the year and showed low reflectance in visible bands due to large amounts of remaining soot.

Table 2
Detection rates of burned areas in different size class categories.

	Burned area patch size (km^2)							
	<10	10–20	20–35	35–60	60–100	100–150	150–250	>250
Number of fires	144	64	48	39	31	19	16	14
Number of fires detected	31	27	23	30	24	16	16	13
Percent detected	22	42	48	77	77	84	100	93

4. Discussion

Our goals were twofold. First, we aimed to estimate changes in burned area before and after the precipitous declines in livestock caused by socioeconomic changes following the breakdown of the Soviet Union. Second, we wanted to develop a method to map burned areas from AVHRR data suitable for the parts of the world for which only data from CLASS were available. Both goals were met successfully.

The main finding from our study was a dramatic increase in burned areas in the arid grasslands of southern Russia starting in the late 1990s (Fig. 6). The area burned each year jumped from almost no fires in the 1980s to large-scale burning, covering up to 20% of study area in a single year after the mid-1990s. Since 1998, on average 1381 km^2 burned per year (9% of the study area, Fig. 9). At this rate, the entire area will burn every 11 years. Fires occurred almost exclusively during the driest season of the year (Carmona-Moreno et al., 2005). Unfortunately, no data on lightning occurrences and dry thunderstorms exist for the area, but our field experience suggests that they are rather rare. Thus we assume that most of the fires are human-caused, resulting from transportation, mainly to and from local herding enterprises, hunting activities, including illegal poaching for indigenous saiga antelope (*Saiga tatarica*), and carelessness (e.g., widespread use of old machinery, smoking, etc.). There is no history of grassland burning for pasture management in the study area (Y. Arylov, personal communication).

4.1. Burned area trends, vegetation, grazing, and socioeconomic changes

The abrupt increase in burned areas that we observed followed a sharp decrease in livestock abundance around the time of breakdown of Soviet Union in 1991. We suggest that the main mechanism leading to the increase in fires was the removal of livestock, predominantly sheep. Reduced disturbance by livestock allowed vegetation to recover, and caused a gradual increase in biomass and fuel connectivity. Grass-dominated vegetation communities (*Stipa* spp.) have increased particularly rapidly (Neronov, 1998). Our results suggest that this recovery of grasslands led to an increase of the amount of dry litter that permitted the consequent significant increase in burning.

Increase in burned areas was also concomitant with the reduction of fire suppression activities in Russia, resulting from economic hardship after the breakdown of Soviet Union in 1991, and the major economic crisis of 1998 (Shvidenko & Goldammer, 2001).

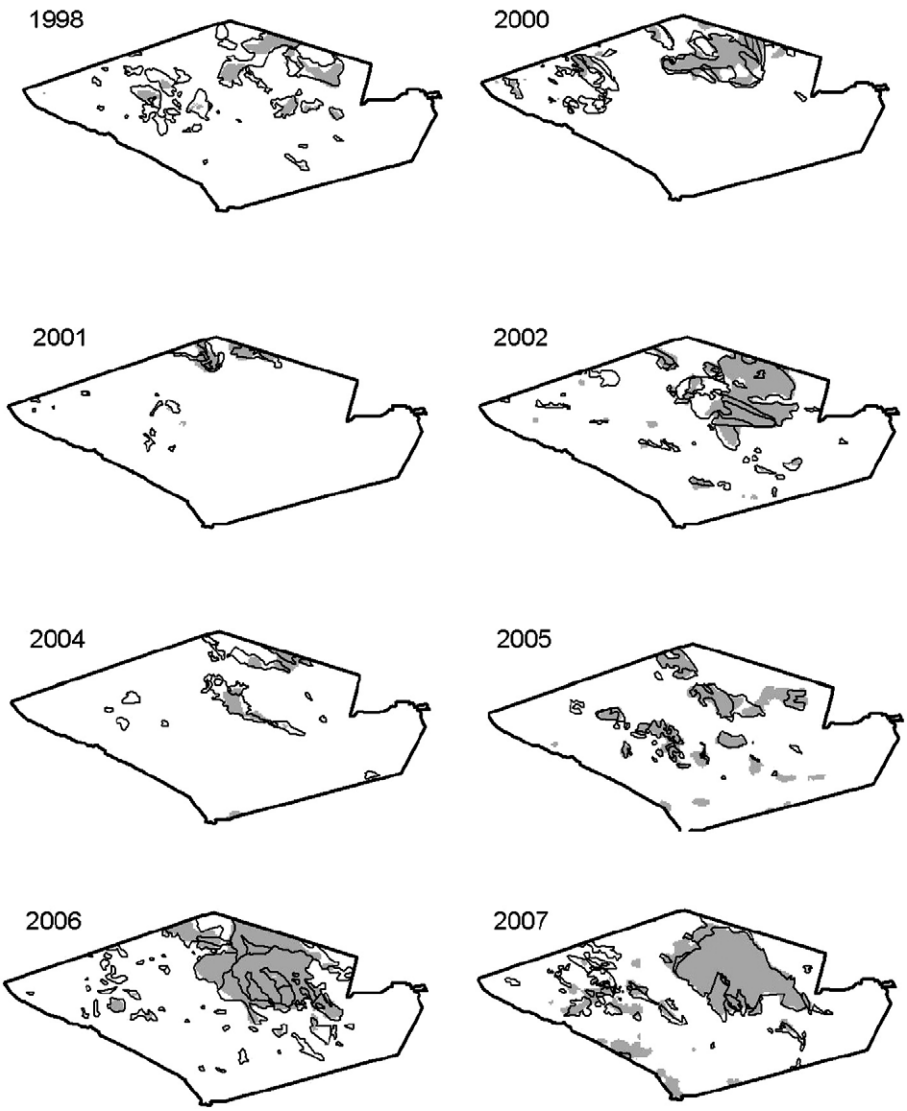

Fig. 9. Burned area mapped for selected years with high fire activity. Gray shading — AVHRR-based burned area maps, black outlines — validation burned area maps (1998 — RESURS-based, others — MODIS-based).

Unemployment caused an increase in the number of visits by locals to the steppe in search of other sources of income. Burning was used to assist poaching of the endangered saiga antelope and led to near obliteration of the last population of saiga in European Russia (Lushchekina & Struchkov, 2001). Official burned areas statistics were only available after 2002. The trends in the burned area statistics correlated well with our AVHRR-based estimates, but official statistics highly underestimated the area burned. Underestimation of fires in governmental data is due to the fact that only fires that were actively suppressed were included in official statistics (Soja et al., 2004).

The strong increase of annual burned area in late 1990s in our study region is similar to other parts of the grasslands of Central Asia and Mongolia. Being part of the Soviet block, these countries showed similar socioeconomic changes and declines in livestock numbers. Though fire data are scarce for Central Asia, there has been a 6-fold increase in steppe and forest fires in Mongolia between the periods of 1985–1995 and 1996–1997 (Erdenesaikhan & Erdenetuya, 1999; Velsen-Zerweck, 2002), similar to the pattern found in our study.

The area that burned most often occurred in a strictly-protected nature reserve (Chernye Zemli Zapovednik) established in 1990, which obtained Biosphere Reserve status in 1993, and covers 1220 km^2 (6% of the study area). The reserve allows research, conservation efforts, and education, but prohibits any other human activities, like livestock grazing or haymaking. The extra protection may have facilitated fuel buildup in the protected area. Together with the livestock declines in the surrounding areas, this may have caused increasing numbers of fires of medium and large size. Although there is no 'let burn' policy in Russia's protected areas, according to our estimation, the reserve burned almost entirely in 2000, 2002, 2006, and 2007, most likely due to the lack of funds for effective fire suppression.

4.2. Satellite data limitations

The only satellite dataset with annual data records spanned from 1985 until present that was available for southern Russia was CLASS-type AVHRR data. Despite the limitations of CLASS-type AVHRR data, we were able to develop a method to map burned areas and to detect long-term trends in annual burned area. However, our accuracy assessment highlighted the limitations of the available coarse-resolution satellite data. We could not use burned area mapping algorithms that require multiple (>2) images for a given year due to the lack of good data in the archives, excessive cloud cover, as well as geometric and radiometric artifacts. In our study area, daily AVHRR data that could be composited were not collected by local stations until the late 1990s. We suggest that the lack of data is largely responsible for the reported classification accuracies, and higher accuracies could have been obtained with if daily acquisitions were available. However, despite its limitations, AVHRR data often provides the only means possible to reconstruct dense time series of burned area estimates for long time spans, prior to the launch of MODIS in 2000. Other remote sensing data, while providing better spectral and spatial resolutions, lack temporal resolution, spatial coverage, and the long-term data record necessary to give clear answer to the question of how burned area changed throughout the recent 20+ years. This is especially true for those regions of the world where remote sensing data records are sparse due to poor archiving or lack of acquisitions. Recent developments in remote sensing data distribution policy, such as the 'freeing' of the Landsat data archives, may make it possible to map burned areas with high resolution in time and space. However, we caution that many areas of the world have acquisition gaps, and methods like the one we present here will be needed to estimate burned area trends for long time series. It would be necessary though to acquire independent fire training and validation data for each study area since our decision trees are specific to our study area and the AVHRR images that we used.

4.3. Validation of the burned area estimates and the burned area mapping approach

Our study dealt with a particularly long time series of satellite observations and various satellite sources were used for validation based on their availability. Though the accuracy of the estimates derived in this study was moderate, similar accuracies were found in comparable environments by studies using better data and more advanced methodology (Roy & Boschetti, 2009). Differences among the imagery used for validation may have resulted in some inconsistencies in the reported accuracy rates, which we could not quantify. Generally, the dataset with highest temporal frequency (i.e., MODIS) was best suited to delineation burned areas for our validation dataset, followed by less frequent, but spatially more detailed Landsat/TM, and finally the only data available for late 1990s (i.e., RESURS/MSU-SK).

Our analysis of the fire season with MODIS active fire data showed that a few fires could have occurred after the dates of our AVHRR images, but burned areas potentially missed were in all likelihood negligible. Our conclusion that fires were essentially absent before 1998 was also supported by our test of the transferability of the decision trees to years for which no training data for burned areas were available. On average 42% of the burned areas detected with full training data were still detected when training data for a given year were omitted. That suggests that even if our visual interpretation of fires in the AVHRR data prior to 1998 missed fires erroneously, our models would have still captured a considerable portion of them.

We found that the largest fires captured up to 70% of the total area burned in a given year (Fig. 10). Burned area classifications in Southern California (Minnich, 1983), the Intermountain West (Knapp, 1998), Mongolia (Erdenesaikhan and Erdenetuya, 1999) and Australia (Yates et al., 2008) found similar pattern with the most of the burned area attributed to few large contiguous burns. We caution though, that the share of large burned areas may have been overestimated due to the low resolution bias of AVHRR data, resulting from the 1.1×1.1 km pixel size (Boschetti et al., 2004), and our use of a majority filter. Omission of small burned areas with AVHRR data is especially critical in mosaic environments representative of crop production systems (Laris, 2005). We cannot rule out that fires were just as frequent prior to 1998, but of such small size that AVHRR missed them all (Table 2). However, this explanation for the observed increase in burned area is highly unlikely. First, size class analysis with higher-resolution MODIS data during the years since 2000, when fires were widespread (Table 2) showed a clear dominance of large fires (Fig. 7), supported by the contiguous nature of grassland vegetation and the absence of crop production. And second, comparable rates of burning expressed as much smaller fires would require much more dense population (to provide ignitions, but also to suppress fires before they got large) or fine patterns of land use (to prevent fires from getting large). Neither was present in the study area historically.

Lastly, our finding that there was essentially no fire prior to 1998 is supported by the only other remote sensing study in the study area. A change detection for 1989 to 1998 by Hoelzel et al. (2002) did not mention any burned areas as well. Though not quantified, sudden and vast increase in burning in our study area after the mid-1990s has also been mentioned in other studies (Shilova et al., 2007) and is corroborated by members of local communities and other scientists working in the area (Bakinova T.I., Dzhapova R.R., Neronov V.V., personal communications).

4.4. Concluding remarks

Our study provides one of the first estimates of burned area trends for the arid grasslands of Central Asia, and represents one of the longest burn area time series obtained using remote sensing here and elsewhere in the world. Drastic socioeconomic changes often lead to

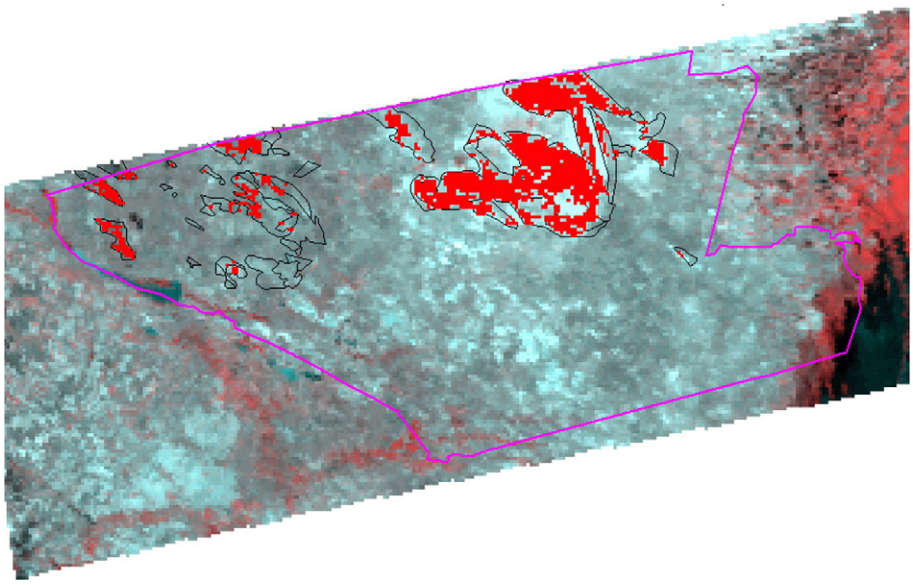

Fig. 10. An example of AVHRR-based burned area map for year 2000 (red polygons) comparing with MODIS-derived burned area validation data (outlined in black) shown on top of the AVHRR image from Aug 1, 2000. The boundary of analysis region is shown in magenta.

changes of a particular disturbance agent. In arid grasslands, the decline in grazing might result in the transition of the ecosystem to the different state. However, changes in vegetation due to reduced grazing likely lead to the substitution of grazing by fire as the main disturbance. Interestingly, the replacement of the disturbance agents did not occur immediately, but exhibited a time lag. Knowing the time lag between disturbances is important in order to make accurate predictions, and we speculate that fire may again decline given continuing restoration of livestock numbers returning to their historic highs (Fig. 1). Whether we are seeing recovery of the ecosystem in the long term or transition to a new state remains a question.

Acknowledgements

We gratefully acknowledge support for this research by the NASA Land-Cover and Land-Use Change Program, the National Geographic Society, and by a NASA Earth System Science Dissertation Fellowship for M. Dubinin (07-Earth07F-0053). We also thank the R&D Center Scanex (Moscow, Russia) for providing RESURS imagery. We thank Dr. Monica Turner and three anonymous reviewers for very helpful and constructive comments.

References

Akiyama, T., & Kawamura, K. (2007). Grassland degradation in China: Methods of monitoring, management and restoration. *Grassland Science*, *53*, 1—17.

Archer, S., Schimel, D. S., & Holland, E. A. (1995). Mechanisms of shrubland expansion — Land-use, climate or CO_2. *Climatic Change*, *29*, 91—99.

Archibald, S., & Bond, W. J. (2004). Grazer movements: Spatial and temporal responses to burning in a tall-grass African savanna. *International Journal of Wildland Fire*, *13*, 377—385.

Arino, O., Piccolini, I., Kasischke, E., Siegert, F., Chuvieco, E., Martin, M. P., et al. (2001). Methods of mapping burned surfaces in vegetation fires. In F. J. Ahern, J. G. Goldammer, & C. O. Justice (Eds.), *Global and regional vegetation fire monitoring from space: planning a coordinated international effort (pp. 227–255)*. : The Haghe SPB Academic Publishing.

Bahre, C. J. (1991). A legacy of change: Historic human impact on vegetation of the Arizona borderlands. : Tucson University of Arizona Press.

Barbosa, P. M., Gregoire, J. -M., & Pereira, J. M. C. (1999). An algorithm for extracting burned areas from time series of AVHRR GAC data applied at a continental scale. *Remote Sensing of Environment*, *69*, 253—263.

Bond, W. J., & van Wilgen, B. W. (1996). *Fire and plants.* London: Chapman and Hall.

Boschetti, L., Flasse, S. P., & Brivio, P. A. (2004). Analysis of the conflict between omission and commission in low spatial resolution dichotomic thematic products: The Pareto Boundary. *Remote Sensing of Environment*, *91*, 280—292.

Bowman, D., Zhang, Y., Walsh, A., & Williams, R. J. (2002). Experimental comparison of four remote sensing techniques to map tropical savanna fire-scars using Landsat-TM imagery. *Conference on Fire and Savanna Landscapes in Northern Australia* (pp. 341—348). Australia: Darwin.

Breiman, L. (1984). *Classification and regression trees.* Belmont, Calif.: Wadsworth International Group.

Breiman, L. (1996). Bagging predictors. *Machine Learning*, *24*, 123—140.

Brooks, K., & Gardner, B. (2004). Russian agriculture in the transition to a market economy. *Economic Development and Cultural Change*, *52*, 571—586.

Brooks, M. L., D'Antonio, C. M., Richardson, D. M., Grace, J. B., Keeley, J. E., DiTomaso, J. M., et al. (2004). Effects of invasive alien plants on fire regimes. *BioScience*, *54*, 677—688.

Burcher, C. L., Valett, H. M., & Benfield, E. F. (2007). The land-cover cascade: Relationships coupling land and water. *Ecology*, *88*, 228—242.

Carmona-Moreno, C., Belward, A., Malingreau, J. P., Hartley, A., Garcia-Alegre, M., Antonovskiy, M., et al. (2005). Characterizing interannual variations in global fire calendar using data from Earth observing satellites. *Global Change Biology*, *11*, 1537—1555.

Chuvieco, E., Englefield, P., Trishchenko, A. P., & Luo, Y. (2008). Generation of long time series of burn area maps of the boreal forest from NOAA-AVHRR composite data. *Remote Sensing of Environment*, *112*, 2381—2396.

CIESIN, & CIAT (2005) Gridded Population of the World Version 3 (GPWv3): Population Density Grids. Palisades, NY; Available at http://sedac.ciesin.columbia.edu/gpw. Last accessed: 06.28.2009: Socioeconomic Data and Applications Center (SEDAC), Columbia University.

CIESIN, FAO, & CIAT (2005) Gridded Population of the World: Future Estimates, 2015 (GPW2015): Population Density Grids. Palisades, NY; Available at http://sedac.ciesin.columbia.edu/gpw. Last accessed: 06.28.2009: Socioeconomic Data and Applications Center (SEDAC), Columbia University.

Congalton, R. G. (1996). Accuracy assessment: a critical component of land cover mapping. In J. M. Scott, T. H. Tear, & F. W. Davis (Eds.), *Gap analysis: a landscape approach to biodiversity planning* (pp. 119—131). Bethesda, Maryland American Society for Photogrammetry and Remote Sensing.

Congalton, R. G., & Green, K. (1998). Assessing the accuracy of remotely sensed data: Principles and practices. CRC Press.

Csiszar, I., Justice, C. O., Mcguire, A. D., Cochrane, M. A., Roy, D. P., Brown, F., et al. (2004). Land use and fires. In G. A. Gutman (Ed.), *Land change science: Observing, monitoring, and understanding trajectories of change on the earth's surface*. Kluwer Academic Publishers.

Csiszar, I., Denis, L., Giglio, L., Justice, C. O., & Hewson, J. (2005). Global fire activity from two years of MODIS data. *International Journal of Wildland Fire*, *14*, 117—130.

Diamond, J. (2001). Ecology: Dammed experiments! *Science*, *294*, 1847—1848.

Erdenesaikhan, N., & Erdenetuya, M. M. (1999). Forest and steppe fire monitoring in Mongolia using satellite remote sensing. *International Forest Fire News*, *21*, 71—74.

Friedl, M. A., & Brodley, C. E. (1997). Decision tree classification of land cover from remotely sensed data. *Remote Sensing of Environment*, *61*, 399—409.

Giglio, L., van der Werf, G. R., Randerson, J. T., Collatz, G. J., & Kasibhatla, P. (2006). Global estimation of burned area using MODIS active fire observations. *Atmospheric Chemistry and Physics*, *6*, 957—974.

Golub, V. B. (1994). The desert vegetation communities of the Lower Volga Valley. *Feddes Repertorium*, *105*, 499—515.

Gong, P., Pu, R. L., Li, Z. Q., Scarborough, J., Clinton, N., & Levien, L. M. (2006). An integrated approach to wildland fire mapping of California, USA using NOAA/AVHRR data. *Photogrammetric Engineering and Remote Sensing*, *72*, 139—150.

Hansen, M. C., Defries, R. S., Townshend, J. R. G., & Sohlberg, R. (2000). Global land cover classification at 1 km spatial resolution using a classification tree approach. *International Journal of Remote Sensing*, *21*, 1331—1364.

Hawbaker, T. J., Radeloff, V. C., Syphard, A. D., Zhu, Z. L., & Stewart, S. I. (2008). Detection rates of the MODIS active fire product in the United States. *Remote Sensing of Environment*, *112*, 2656—2664.

Hoelzel, N., Haub, C., Ingelfinger, M. P., Otte, A., & Pilipenko, V. N. (2002). The return of the steppe: Large-scale restoration of degraded land in southern Russia during the post-Soviet era. *Journal for Nature Conservation (Jena)*, *10*, 75—85.

Justice, C. O., Vermote, E., Townshend, J. R. G., Defries, R., Roy, D. P., Hall, D. K., et al. (1998). The Moderate Resolution Imaging Spectroradiometer (MODIS): Land remote sensing for global change research. *IEEE Transactions on Geoscience and Remote Sensing*, *36*, 1228—1249.

Knapp, P. A. (1998). Spatio-temporal patterns of large grassland fires in the Intermountain West, USA. *Global Ecology and Biogeography*, *7*, 259—272.

Kroonenberg, S. B., Rusakov, G. V., & Svitoch, A. A. (1997). The wandering of the Volga delta: A response to rapid Caspian sea-level change. *Sedimentary Geology*, *107*, 189—209.

Kučera, J., Yasuoka, Y., & Dye, D. G. (2005). Creating a forest fire database for the Far East of Asia using NOAA/AVHRR observation. *International Journal of Remote Sensing*, *26*, 2423—2439.

Kuemmerle, T., Hostert, P., Radeloff, V. C., Perzanowski, K., & Kruhlov, I. (2007). Post-socialist forest disturbance in the Carpathian border region of Poland, Slovakia, and Ukraine. *Ecological Applications*, *17*, 1279—1295.

Kurinova, Z. S., & Belousova, Z. N. (1989). *Effective use of forage resources.* Elista: Kalmyk book publishing.

Lambin, E. F., & Geist, H. (2006). Land-use and land-cover change: Local processes and global impacts. Springer.

Laris, P. S. (2005). Spatiotemporal problems with detecting and mapping mosaic fire regimes with coarse-resolution satellite data in savanna environments. *Remote Sensing of Environment*, *99*, 412—424.

Lee, D. S., Storey, J. C., Choate, M. J., & Hayes, R. W. (2004). Four years of Landsat-7 on-orbit geometric calibration and performance. *IEEE Transactions on Geoscience and Remote Sensing*, *42*, 2786—2795.

Liedloff, A. C., Coughenour, M. B., Ludwig, J. A., & Dyer, R. (2001). Modelling the trade-off between fire and grazing in a tropical savanna landscape, northern Australia. *Environment International*, *27*, 173—180.

Lushchekina, A. A., & Struchkov, A. (2001). The saiga antelope in Europe: Once again on the brink? *The Open Country*, *3*, 11—24.

Mack, R. N., & Thompson, J. N. (1982). Evolution in steppe with few large, hooved mammals. *American Naturalist*, *119*, 757—773.

Maggi, M., & Stroppiana, D. (2002). Advantages and drawbacks of NOAA-AVHRR and SPOT-VGT for burnt area mapping in a tropical savanna ecosystem. *Canadian Journal of Remote Sensing*, *28*, 231—245.

Meyn, A., White, P. S., Buhk, C., & Jentsch, A. (2007). Environmental drivers of large, infrequent wildfires: The emerging conceptual model. *Progress in Physical Geography*, *31*, 287—312.

Miettinen, J., Langner, A., & Siegert, F. (2007). Burnt area estimation for the year 2005 in Borneo using multi-resolution satellite imagery. *International Journal of Wildland Fire*, *16*, 45—53.

Minnich, R. A. (1983). Fire mosaics in Southern California and Northern Baja California. *Science*, *219*, 1287—1294.

Neronov, V. V. (1998). Antropogenic grasslands encroachment of desert pastures of North-Western Precaspian plains.*Successes of Modern Biology*, *118*, 597—612 (in Russian).

Pereira, J. M. C. (1999). A comparative evaluation of NOAA/AVHRR vegetation indexes for burned surface detection and mapping. *IEEE Transactions on Geoscience and Remote Sensing*, *37*, 217—226.

Pu, R. L., Li, Z. Q., Gong, P., Csiszar, I., Fraser, R., Hao, W. M., et al. (2007). Development and analysis of a 12-year daily 1-km forest fire dataset across North America from NOAA/AVHRR data. *Remote Sensing of Environment*, *108*, 198—208.

Pyne, S. J. (1984). *Introduction to wildland fire.* New York: John Wiley and Sons.

Razafimpanilo, H., Frouin, R., Iacobellis, S. F., & Somerville, R. C. J. (1995). Methodology for estimating burned area from AVHRR reflectance data. *Remote Sensing of Environment*, *54*, 273—289.

ROSSTAT (2003). Agriculture in Republic of Kalmykia. *Kalmykia in numbers (in Russian)*. Elista.

ROSSTAT (2007). Agriculture in Republic of Kalmykia. *Kalmykia in numbers (in Russian)*. Elista.

Roy, D. P., & Boschetti, L. (2009). Southern Africa validation of the MODIS, L3JRC, and GlobCarbon burned-area products. *IEEE Transactions on Geoscience and Remote Sensing*, *47*, 1032—1044.

Saiko, T., & Zonn, I. (1997). Europe's first desert. In M. Glantz, & I. Zonn (Eds.), *Scientific, environmental and political issues in the circum-Caspian region* (pp. 141—144). Boston and London Kluwer Academic Publishers: Dordrecht.

Shilova, S. A., Neronov, V. V., Kasatkin, M. V., Savinetskaya, L. E., & Chabosvky, A. V. (2007). Modern burning in semi-deserts of Southern Russia: Influence on vegetation and rodents populations. *Uspekhi Sovremennoi Biologii*, *127*, 372—386.

Shvidenko, A., & Goldammer, J. G. (2001). Fire situation in Russia. *International Forest Fire News*, *24*, 41—59.

Soja, A. J., Sukhinin, A. I., Cahoon, D. R., Shugart, H. H., & Stackhouse, P. W. (2004). AVHRR-derived fire frequency, distribution and area burned in Siberia. *International Journal of Remote Sensing*, *25*, 1939—1960.

Song, C., Woodcock, C. E., Seto, K. C., Lenney, M. P., & Macomber, S. A. (2001). Classification and change detection using Landsat TM data: When and how to correct atmospheric effects? *Remote Sensing of Environment*, *75*, 230—244.

Stohl, A., Berg, T., Burkhart, J. F., Fjaeraa, A. M., Forster, C., Herber, A., et al. (2007). Arctic smoke — Record high air pollution levels in the European Arctic due to agricultural fires in Eastern Europe in spring 2006. *Atmospheric Chemistry and Physics*, *7*, 511—534.

Stroppiana, D., Tansey, K., Gregoire, J. M., & Pereira, J. M. C. (2003). An algorithm for mapping burnt areas in Australia using SPOT-VEGETATION data. *IEEE Transactions on Geoscience and Remote Sensing*, *41*, 907—909.

Sukhinin, A. I., French, N. H. F., Kasischke, E. S., Hewson, J. H., Soja, A. J., Csiszar, I. A., et al. (2004). AVHRR-based mapping of fires in Russia: New products for fire management and carbon cycle studies. *Remote Sensing of Environment*, *93*, 546—564.

Tansey, K., Gregoire, J. M., Stroppiana, D., Sousa, A., Silva, J., Pereira, J. M. C., et al. (2004). Vegetation burning in the year 2000: Global burned area estimates from SPOT VEGETATION data. *Journal of Geophysical Research-Atmospheres*, *109*.

van der Werf, G. R., Randerson, J. T., Giglio, L., Collatz, G. J., Kasibhatla, P. S., & Arellano, A. F. (2006). Interannual variability in global biomass burning emissions from 1997 to 2004. *Atmospheric Chemistry and Physics*, *6*, 3423—3441.

Velsen-Zerweck, M.v. (2002). Socio-economic causes of forest loss in Mongolia. *Sozialökonomische Schriften zur Ruralen Entwicklung* (p. xxi + 357 pp.).

Vinogradov, B.V. (1995). Forecasting dynamics of deflated sands of Black Lands, Kalmykia using aerial photography. In N. Zonn I.S., V.M. (Ed.) *Biota and Environment of Kalmykia* (pp. 259–268). Moscow, Elista (in Russian).

Walter, H., & Box, E. (1983). Overview of Eurasian continental deserts and semideserts. *Ecosystems of the world* (pp. 3—269). Amsterdam Elsevier.

Yates, C. P., Edwards, A. C., & Russell-Smith, J. (2008). Big fires and their ecological impacts in Australian savannas: Size and frequency matters. *International Journal of Wildland Fire*, *17*, 768—781.

Zhang, K., Yu, Z., Li, X., Zhou, W., & Zhang, D. (2007). Land use change and land degradation in China from 1991 to 2001. *Land Degradation & Development*, *18*, 209—219.

Zonn, S.V. (1995). Desertification of nature resources in Kalmykia during last 70 years and protection measures. *Biota and Environment of Kalmykia* (pp. 12–52). Moscow, Elista (in Russian).